Pergamon

Journal of Structural Geology, Vol. 18, No. 7, pp. 871 to 889, 1996

0191-8141/96 $15.00 + 0.00

PII: S0191-8141(96)00014-4

# Superimposed fabrics due to reversal of shear sense: an example from the Bergen Arc Shear Zone, western Norway

OLE PETTER WENNBERG

Institute of Geology, University of Bergen, Allégt.41, 5007 Bergen, Norway

(*Received* 12 *June* 1995; *accepted in revised form* 30 *January* 1996)

**Abstract**—A profile through the upper margin of a large scale ductile shear zone (the Bergen Arc Shear Zone, western Norway) has been studied in detail. Within the shear zone, asymmetric structures indicate dextral or top-to-NW movement, which is interpreted as representing late or post-Caledonian extensional tectonics. The hanging-wall of the shear zone is characterised by kinematic indicators, such as shear bands associated with curved or inclined foliation and asymmetric boudins, indicating sinistral or top-to-SE movements. These are interpreted as related to thrusting during the Caledonian Orogeny. The studied profile shows the progressive overprinting of the sinistral structures by the later dextral shear. This first led to a decrease in the obtuse angle between shear bands and the curved/inclined foliation. Subsequently, backfolding of asymmetric boudins in quartz veins occurred, and a composite cleavage developed from shear bands and associated curved/inclined foliation. Dextral asymmetric extensional shear bands were developed at a later stage when the folded quartz veins had attained tight to isoclinal geometries. Copyright © 1996 Elsevier Science Ltd

## INTRODUCTION

Since the late 1970s numerous papers have discussed the development of the internal structures and fabrics in shear zones especially in order to determine the sense of movement between different tectonic units (see Hanmer & Passchier 1991 for review). Most contributions focus on one phase of shear deformation with a constant shear direction. Even in this case, the internal parts of shear zones can show complex geometries due to high shear strain, progressive refolding, strain-partitioning, retrogression etc. Changing shear directions and/or polyphasal deformation may increase the complexity of internal structures in shear zones dramatically. For example, two phases of shear can result in a multitude of configurations resulting from the different orientation of the two shear planes and different shear directions. This paper discusses some aspects of one of the simplest cases, where the shear planes and shear directions were the same, but the senses of shear were opposite during two phases of deformation. The studied field example, the Askvik shore section, near Bergen (western Norway), shows the progressive superimposition of dextral shear on earlier sinistral structures.

Shear bands or asymmetric extensional shear bands associated with curved/inclined foliation are one of the most commonly used structures to determine the sense of shear in shear zones (Hanmer & Passchier 1991). More or less synonymous terms are 'C′' (Berthé *et al.* 1979), 'extensional crenulation cleavage' (Platt & Vissers 1980), 'shear band foliation' (White *et al.* 1980) and 'normal-slip crenulations' (Dennis & Secor 1987). Other structures which are often used include asymmetric boudins (Hanmer 1986, Goldstein 1988). Two major phases of shear deformation with opposite sense of shear affected the Scandinavian Caledonides of western Norway (e.g. Fossen 1992). Favourable conditions along the section described in this paper allow the geometry of progressive reworking and overprinting of shear bands and asymmetric boudins in shear zones of this type to be demonstrated and analysed in detail.

## GEOLOGICAL SETTING

The Caledonian orogen in Scandinavia resulted from the convergence of Laurentia and Baltica in late Ordovician to early Devonian times. During the main orogenic phase (late Silurian/early Devonian), a nappe wedge was established with transport direction mainly towards SE over the margin of Baltica (e.g. Sturt & Thon 1978, Roberts & Sturt 1980). The final continent–continent collision resulted in a thickened crust with high-pressure metamorphism and eclogite formation (e.g. Griffin *et al.* 1985).

During late/post-Caledonian times a major extensional event took place which resulted in thinning of the orogenically thickened crust (Hossack 1984). This late/post-orogenic extensional tectonics is thought to have led to the formation of Devonian basins in western Norway, and to rapid exhumation of the eclogite facies metamorphic rocks (Hossack 1984, Norton 1986, Séranne & Seguret 1987, Andersen & Jamtveit 1990). According to Fossen (1992) the extensional deformation is characterized by two different modes of deformation. Mode 1 deformation involves back-movement of the Caledonian nappes towards NW by reactivation of the Caledonian thrust planes. Extensional deformation fabrics (top-to-W or -NW) overprint the contractional Caledonian structures (top-to-SE) within the reactivated thrust zones. Mode 2 deformation subsequently resulted in the formation of large scale, low-angle extensional shear zones which transected and extended the Baltic Shield and the nappe wedge. The most important of these is the low-angled and west-dipping Nordfjord-Sogn Detachment (Norton 1986). The extensional (top-to-W or -NW) nature of this structure has been demonstrated in several structural analyses (e.g. Chauvet & Séranne 1989, Swensson & Andersen 1991).

Reactivation and overprinting of fabrics developed during the Caledonian orogeny by late/post-orogenic extension have been described in several other localities. In the Ofoten area, in the northern Scandinavian Caledonides, interference between top-to-E and top-to-W fabrics has been described by Rykkelid & Andresen (1994). Crenulation fabrics in mica-rich lithologies related to top-to-W extension are interpreted as representing the folding of an earlier foliation between top-to-E shear bands, where top-to-W shear bands were developed as a late feature during reactivation.

Other features interpreted to represent late/post Caledonian reactivation of an earlier thrust-related fabric are systems of asymmetric late folds with a vergence towards NW to W, often termed back-folds. These NW- to W-verging folds have been described at several places in the southwestern Norwegian Caledonides especially in the décollement zone under the Jotun Nappe (e.g. Naterstad *et al.* 1973, Milnes & Koestler 1985, Fossen & Holst 1995) and in the Sunnfjord region (Skjerlie 1969, Andersen *et al.* 1990). Although the geometry of the back-folds appears consistent, their size varies from millimetre-scale to map-scale with limb lengths of several hundred metres. The general idea is that the foliation developed during the Caledonian top-to-SE thrusting was gently inclined relative to the dècollement zone or shear plane of the later top-to-NW movement. Models for the formation of the back-folds include slip parallel to the foliation, producing reverse slip crenulations (Dennis & Secor 1987, Osmundsen & Andersen 1994, Fossen & Holst 1995), and the foliation oriented in the contractional field of the instantaneous strain ellipse, resulting in buckling (Fossen & Holst 1995). However, none of these works describe localities at which the process of superimposition can be followed and demonstrated in detail, as can be done at the locality described below.

## THE ASKVIK SHORE SECTION

The section described in this paper runs along the northern shore of the Osterfjord, near the hamlet of Askvik, north of Bergen, and is located on the northeastern border of the Bergen Arc System (Fig. 1). The Bergen Arc System (Kolderup & Kolderup 1940) designates a series of rock units around Bergen in western Norway with an arcuate outcrop pattern. Several authors have suggested that the northeastern margin of the Bergen Arc System represents the southward continuation of a branch of the Nordfjord-Sogn Detachment (Norton 1986, 1987, Milnes *et al.* 1988, Séranne *et al.* 1991). Structural observations supporting this hypothesis have been presented by Wennberg & Milnes (1994). The northeastern margin of the Bergen Arc System is marked by a 2–3-km-thick shear zone, dipping 50–60° SW and characterized by asymmetric structures indicative of oblique movements with normal and dextral components. A lineation plunging at approximately 20° in a west–northwest direction is developed in the lower and central parts of the shear zone. In the higher parts the shear direction has a subhorizontal orientation. This shear zone has been called the Bergen Arc Shear Zone (Fossen 1992) and involves parts of three tectonic units: the Western Gneiss Complex, the Kvalsida Gneiss and the Major Bergen Arc zone. The Askvik shore section lies wholly within the Major Bergen Arc zone and crosses the southwestern (upper) margin of the Bergen Arc Shear Zone.

The Major Bergen Arc Zone (MaBA) can be broadly divided into three units. (1) Basic intrusives and extrusives interpreted as a dismembered ophiolite fragment, the Gullfjellet Ophiolite Complex (Furnes *et al.* 1980, Thon 1985), which has U/Pb ages of 489 $\pm$ 3 Ma (plagiogranite) and 486 $+ 6/-2$ Ma (tonalite) (Dunning & Pedersen 1988). (2) The Samnanger Complex east of the Gullfjellet Ophiolite Complex thought to represent a large scale imbricate structure consisting of Lower Palaeozoic metasedimentary schists, with slices of ophiolitic rocks in the west and of basement gneisses in the east (Færseth *et al.* 1977, Thon 1985). (3) The Holdhus and Ulven Groups, consisting of conglomerates, fossilliferous limestones and phyllites of Ashgillan to middle Llandoverian age (Færseth *et al.* 1977, Ryan & Skevington 1976, Reusch 1882). They are separated from the underlying Samnanger Complex and Gullfjellet Ophiolite Complex by a major unconformity, and were deposited after an early phase of deformation which affected these complexes (Sturt & Thon 1976, Færseth *et al.* 1977).

The MaBA is an 8–10 km broad zone in the southeast which becomes dramatically thinner northwestward across Osterøy (Fig. 1). In the studied area, north of Osterøy, the thickness of the MaBA has decreased to less than 1 km. The strongly sheared MaBA rocks in the study area have been divided into two parts (Wennberg & Milnes 1994). The upper part is characterized by garnet–amphibole–mican-schist and garben-schist with kinematic indicators showing a sinistral sense of shear. In contrast, kinematic indicators in the lower part, which consists mostly of phyllite and is within the Bergen Arc Shear Zone, show a dextral sense of shear. In the shear zone, sinistral indicators are only preserved locally in quartz/feldspar-rich lithologies. Since the foliation in the area has a dip of 50°–60° towards SW, the dextral movements represent top-to-NW and the sinistral top-to-SE shear senses. The dextral sense of shear post-dates the sinistral, and the transition zone between these two parts is the main focus of this paper (Fig. 2).

## STRUCTURAL RELATIONS

The Askvik shore section (Fig. 2) displays a continuous profile across the upper margin of the Bergen Arc

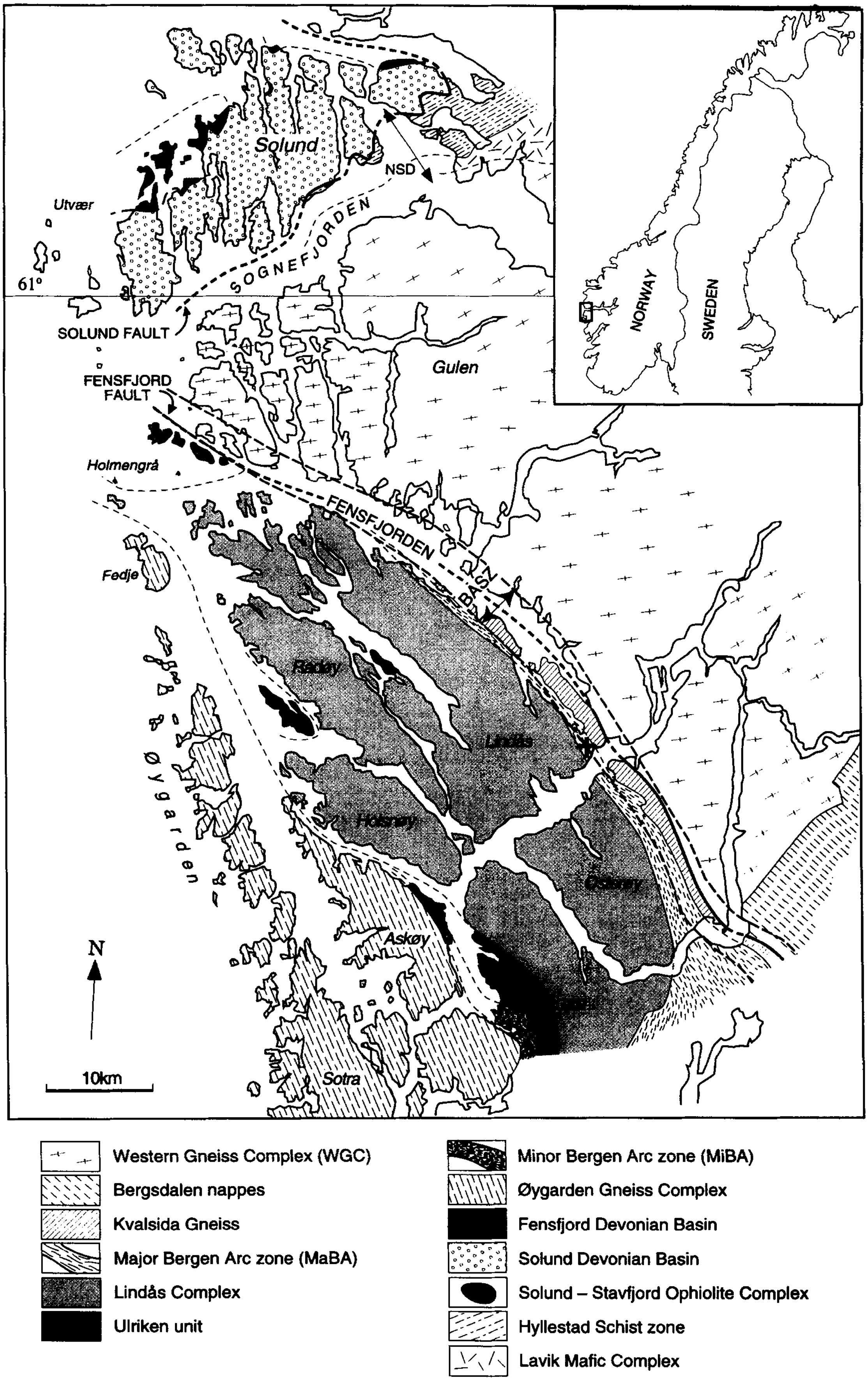


Fig. 1. Simplified geological map of the northern part of the Bergen Arc System. BASZ shows the approximate extent of the Bergen Arc Shear Zone and NSD the Nordfjord-Sogn Detachment. X marks the area studied in detail and shown in Fig. 2.

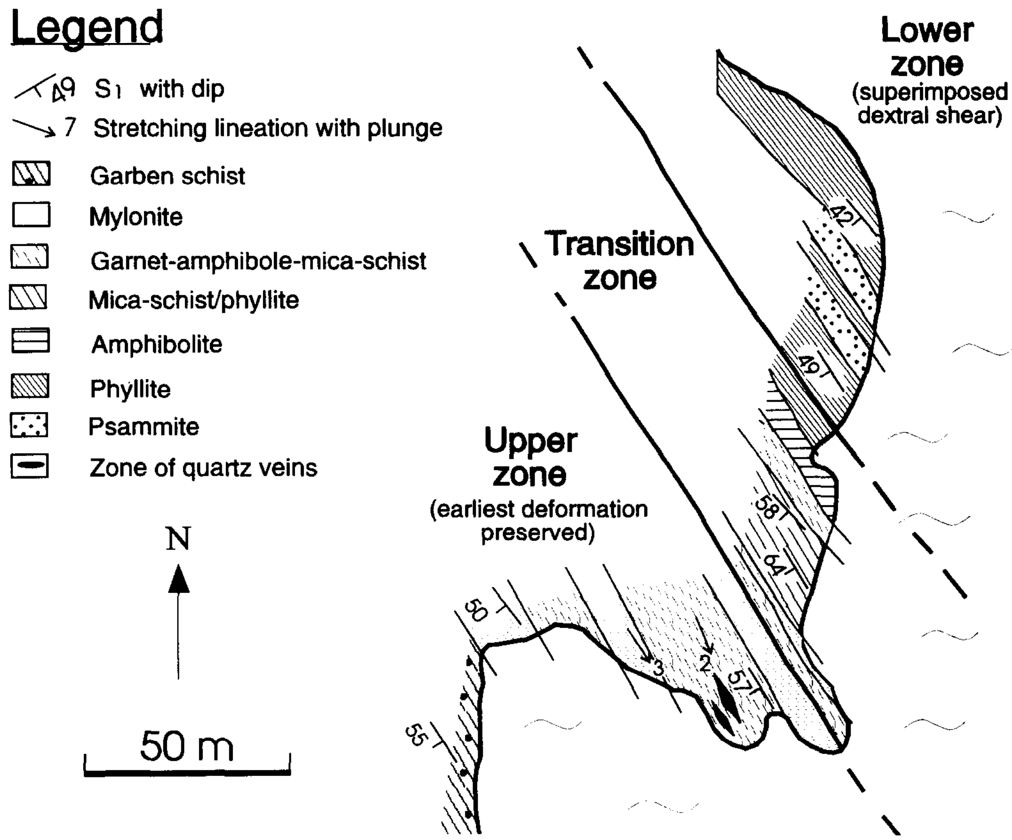


Fig. 2. Geological map of the Askvik shore section with the main structural elements. For location see Fig. 1.

Shear Zone. Based on detailed structural mapping it can be divided into an upper zone showing sinistral sense of shear, a lower zone of dextral shear and an intervening transition zone. As demonstrated below, the dextral movements post-date the sinistral ones. In the following, the structural development along this profile is described from top to bottom, showing the progressive superimposition of dextral shear on the earlier sinistral structures.

*Upper zone—sinistral kinematic indicators*

The upper zone represents the hanging-wall of the Bergen Arc Shear Zone, and the structures here are preserved from the Caledonian top-to-SE thrusting. This zone consists of garben-schist (Garbenschiefer) and garnet–amphibole–mica-schist with thinner zones of psammites, mylonites and phyllonites. In the mica-schists, quartz veins are common, and locally lens-shaped volumes rich in quartz veins occur (>30%). A well defined schistosity in the garben schist is defined by parallel micas and quartz aggregates. Amphibole prisms lie with different orientations within this foliation, and often occur in characteristic bow-tie arrangements. Kinematic indicators are generally not developed within this lithology, and it mainly occurs in the structurally higher part of the profile.

The most important structural elements of the upper zone, with the exception of the garben schist are illustrated in Fig. 3. In centimetre- to metre-thick zones only one planar structure is present, which is termed $S_1$, oriented subparallel to the compositional layering. This fabric tends to be developed in lithologies rich in quartz and feldspar, i.e. in the psammites. The $S_1$ foliation is defined by subparallel orientation of micas, quartz and calcite aggregates, and quartz veins. $S_1$ has a rather constant orientation with a mean strike of 150° and a mean dip of 56° SW (Fig. 4a). A subhorizontal stretching lineation ($L_1$) is developed on the quartz veins and on the $S_1$ foliation. Shear bands ($SB_1$) associated with curved/inclined foliation ($SI_1$) occur in metre- to tens of metre-thick zones between the zones of parallel $S_1$ and quartz veins (Figs. 3 and 5a). These relations tend to be better developed in more mica-rich lithologies. $SI_1$ is sigmoidal and curved, and the orientation is measured in the central relative planar part.

$SI_1$ shows identical features to $S_1$, being defined by parallel micas, quartz/calcite aggregates and quartz veins. The shear bands in contrast, are discontinuous structures, and can be geometrically characterised as small ductile to brittle–ductile shear zones as defined by Ramsay (1980). They normally have a thickness less than 1 mm and a spacing in the range of 5–20 mm. The shear bands are moderately anastomosing, and tend to be enriched in calcite, opaque minerals and micas relative to quartz and feldspar.

The relation between the main structural elements is also indicated by the pole distribution of the different

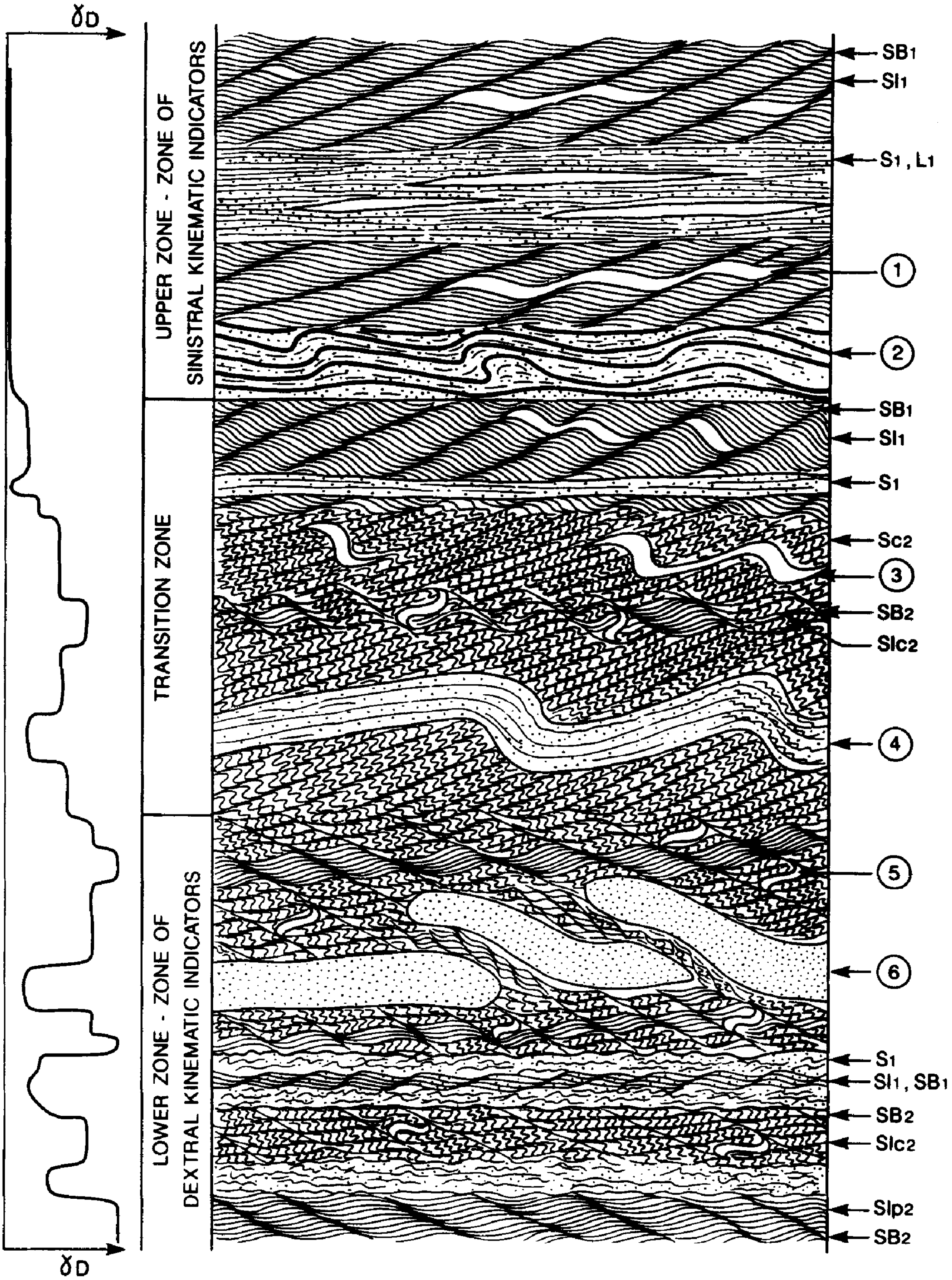


Fig. 3. Schematic structural log of the Askvik shore section (upper margin of the Bergen Arc Shear Zone). Not to scale. (1) Asymmetric pinch-and-swell structure in quartz. (2) Asymmetric folds with sinistral vergence. (3) Back-folding of symmetric pinch-and-swell structure (see Fig. 4d). (4) Asymmetrically folded $S_1$ with dextral vergence. (5) Isoclinally folded quartz boudin (see Fig. 5f). (6) Imbricated psammite band. The curve illustrates the relative amount of superimposed dextral shear strain ($\gamma_D$).

planar structures in Fig. 4(a). The poles to the $SB_1$ and $SI_1$ are grouped in two areas distributed more or less symmetrically around the cluster of $S_1$ poles. The obtuse angle between the $SB_1$ and the $SI_1$ is called $\beta$ here. In this upper zone, $\beta$ is usually between 130 and 150° with a mean of 143.2° (Fig. 6a). The $SI_1$ is inclined 15° to 20° relative to the $S_1$. The relationship between $SB_1$, $SI_1$, $S_1$ and $L_1$ indicates sinistral non-coaxial deformation in map view. Locally, reverse-slip crenulations (Dennis & Secor 1987) are developed, also indicating sinistral shear. In a 4–5-m-thick zone oriented subparallel to the mean $S_1$ consisting of alternating mylonitic and phyllonitic bands, the $S_1$ is folded by complex non-cylindrical folds.

The shear bands control the development of the

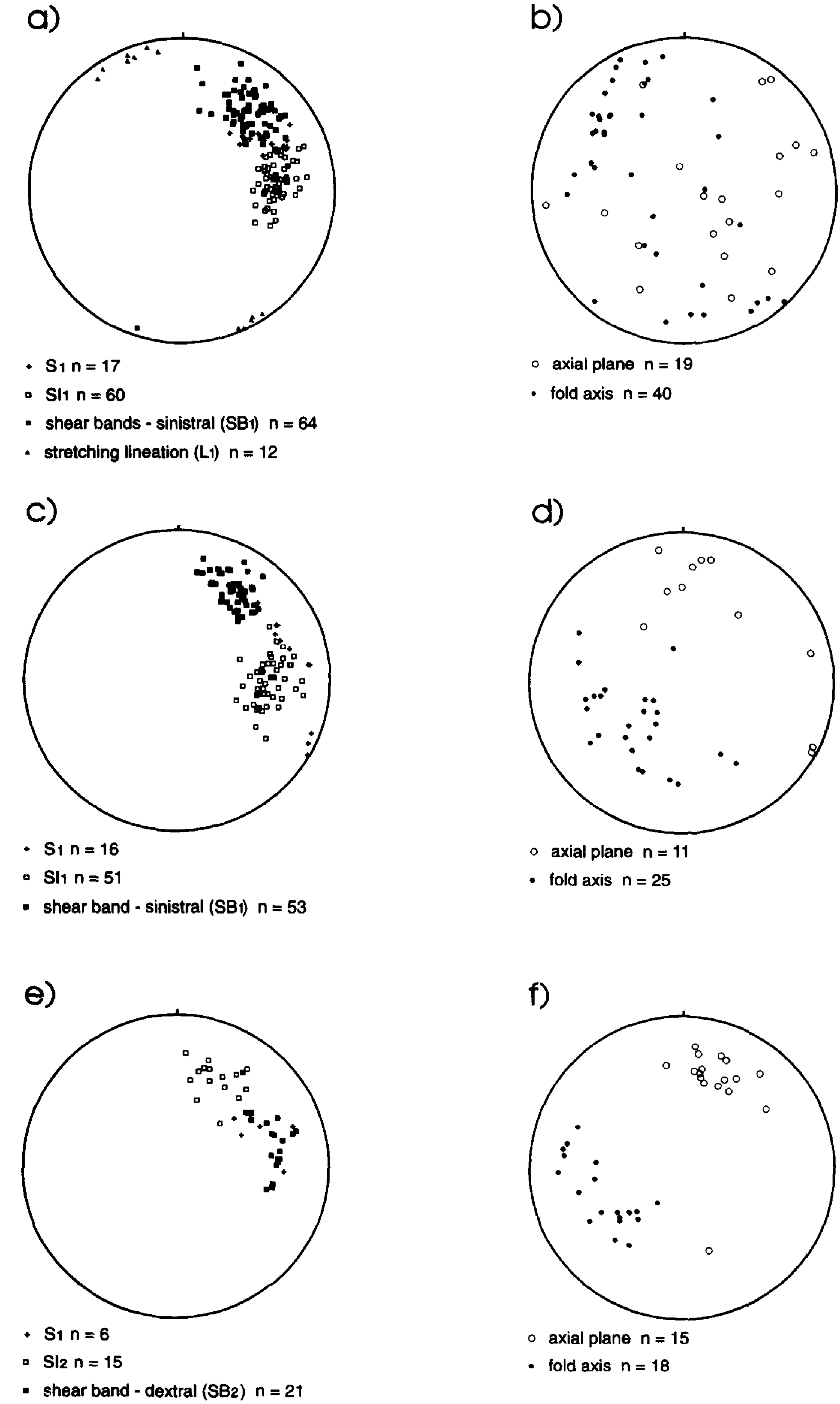


Fig. 4. Stereoplots of structures from the area mapped on Fig. 2. (a) and (b) from the upper zone of sinistral shear, (c) and (d) from the transition zone, (e) and (f) from the lower zone of dextral shear. Equal area projection, lower hemisphere.

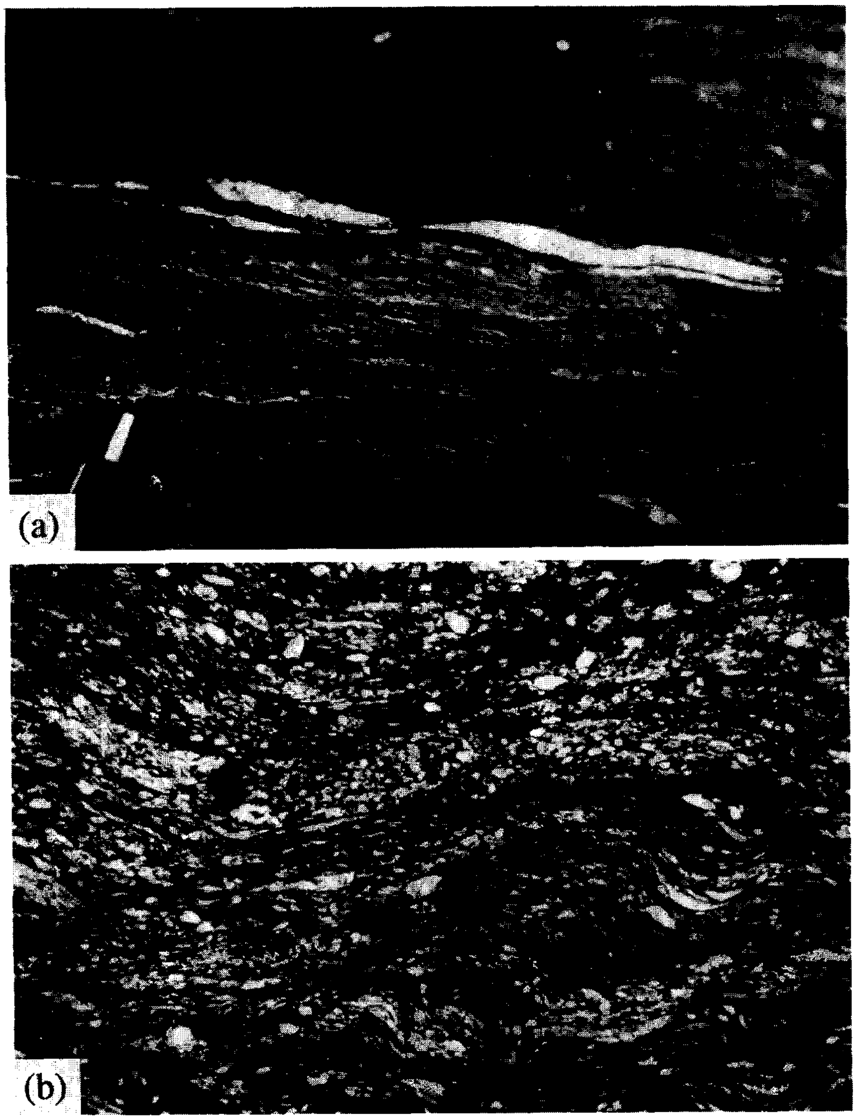

Fig. 5. Characteristic structures from the Askvik shore section. All photos of subhorizontal exposures with SSE to the left. (a) $SB_1$ and $SI_1$ indicating sinistral shear in the upper zone. Same sense of shear is inferred from asymmetric boudins and pinch-and-swell structures. (b) Thin-section of shear bands ($SB_1$) indicating sinistral shear in the transition zone. Dextral verging folds in the lower left part suggest that this fabric has been modified by later dextral shear. (c) Incipient back-folding of quartz lens in a mica-rich matrix showing dextral verging crenulations in the transition zone. (d) Folded quartz lens from the transition zone. The fold is tighter than in (c) due to increased superimposed dextral shear. Note the sinistral asymmetric boudins to the left of the folded lens. (e) Folded quartz vein in the transition zone (similar matrix to the quartz vein shown in c). (f) & (g) Thin-section photographs of composite cleavage ($SI_{C2}$) in the dextral zone. See text for discussion. (h) Shear band ($SB_2$) indicating dextral sense of shear in the lower zone. (i) Detail from (h) showing isoclinally folded quartz vein preserved between the dextral shear bands. Scale of thin-section photos is 10:1.

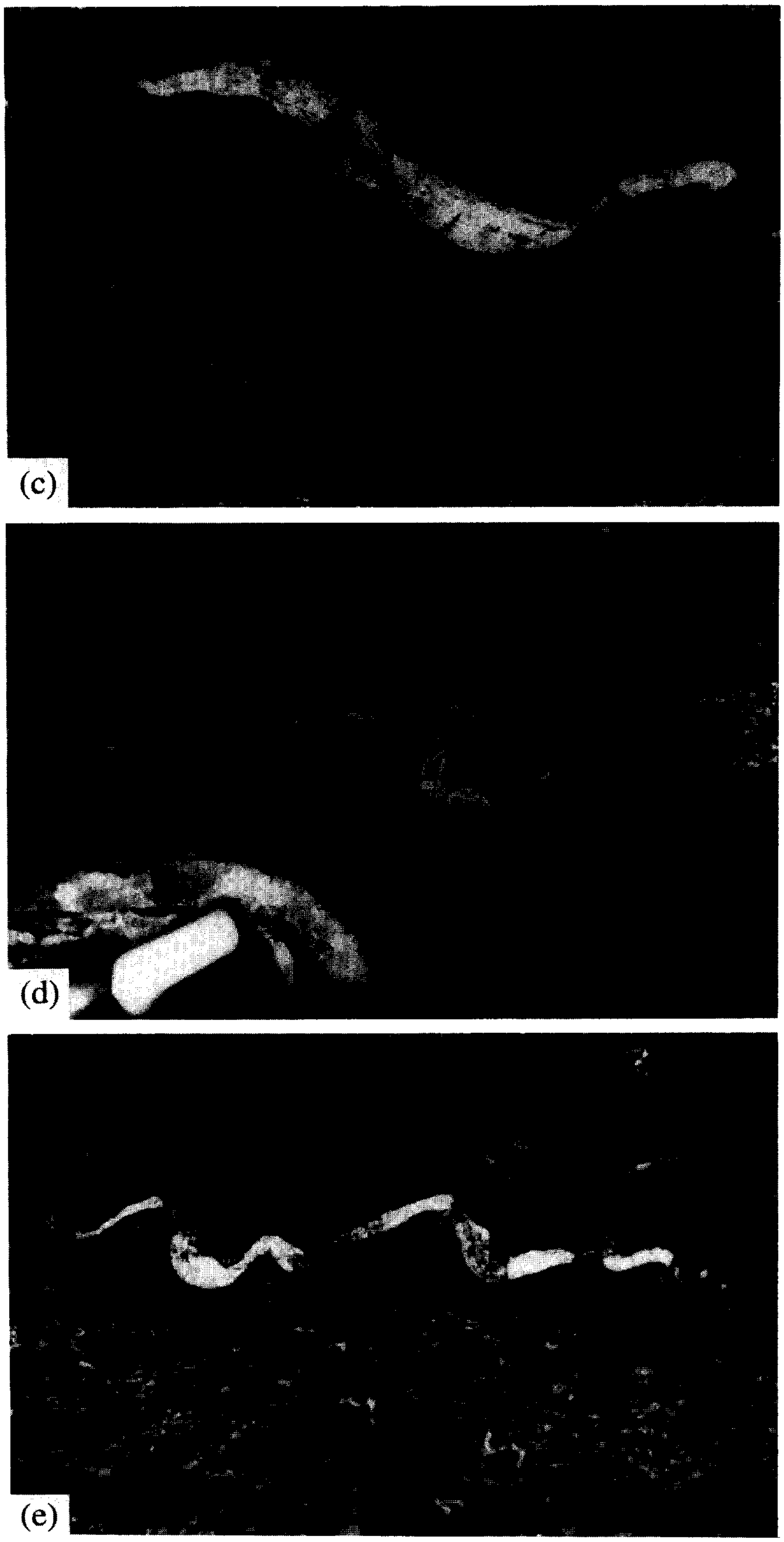


Fig. 5. (*continued*)

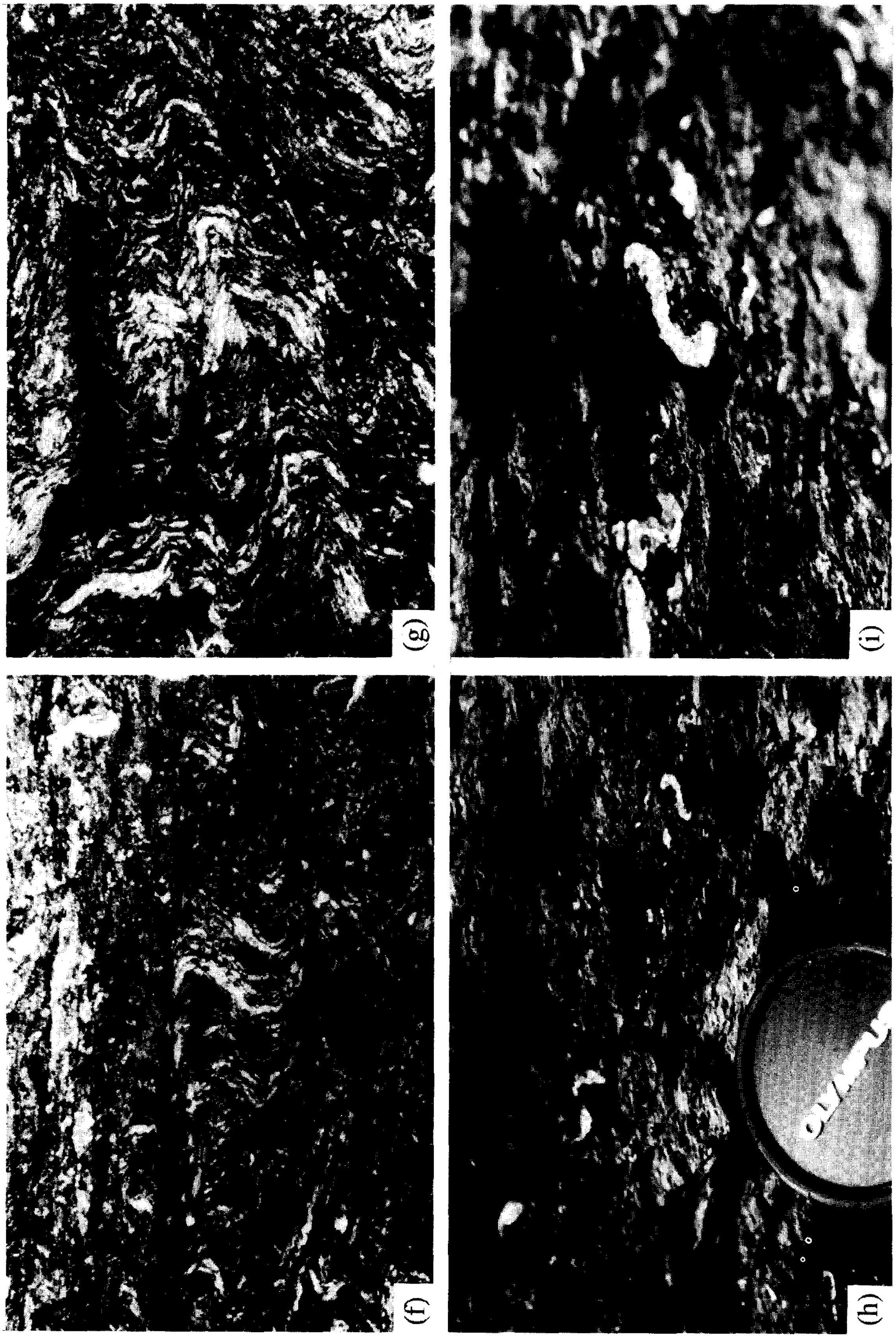


Fig. 5. (*continued*)

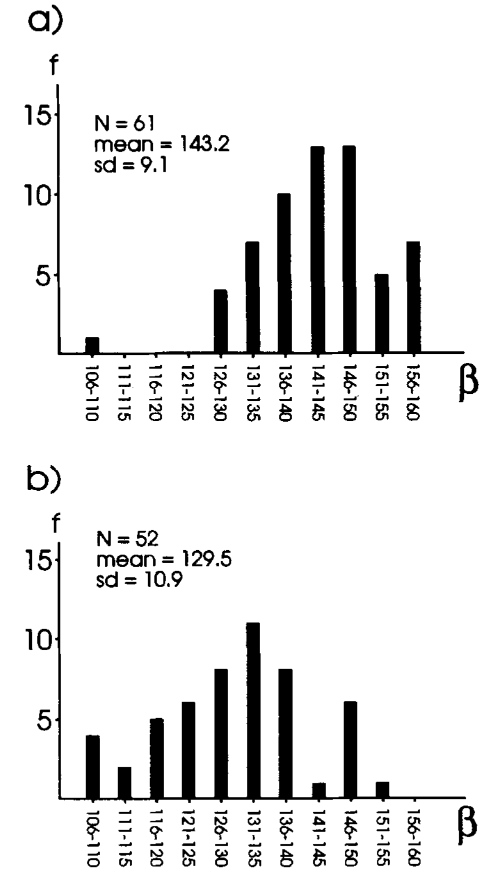


Fig. 6. Frequency of measured angles between shear bands ($SB_1$) and associated curved/inclined foliation ($SI_1$). (a) From the sinistral zone, (b) from the transition zone.

asymmetric boudins and pinch-and-swell structures from which sinistral sense of shear also is inferred (Fig. 5a). The quartz boudins have a slightly sigmoidal shape. The central part of the lenses are inclined relative to the $S_1$ in a similar way to the $SI_1$ foliation, while thin, short tails are bent into parallelism with the shear bands. For the asymmetric pinch-and-swell structures, quartz veins are thinned through, and rotated into parallelism with the shear bands. The pinches are oriented subparallel to the shear bands, while the thicker swells are oriented parallel to the $SI_1$.

In the upper zone the shear plane is constrained by the compositional layering, $S_1$, the $SB_1/SI_1$ intersection and the stretching lineation $L_1$. The $SB_1/SI_1$ intersections and $L_1$ plot close to the average $S_1$ and the angle between them is approximately 90°(Fig. 7a). Mean $S_1$ (150/56 SW) as well as the compositional layering have approximately the same orientation as the plane bisecting the acute angle between the mean shear band and $SI_1$ (148/60 SW). This suggests that the average mylonitic $S_1$ foliation is a good approximation to the shear plane. The shear direction is found as the perpendicular to the $SB_1/SI_1$ intersection within the inferred shear plane. It must be noted that a small inaccuracy, i.e. 55° $\pm$ 3°, in the measurement of the dip of the $SB_1$ and $SI_1$ planes will contribute to a major inaccuracy of $\pm$ 13° for the intersection between these planes and therefore also for the shear direction (Fig. 7c). This inaccuracy has a significant influence on the dispersion of the determined shear directions. Considering this inaccuracy, the mean determined shear direction of 158/10 (trend/plunge) is in accordance with the stretching lineations with a mean of 335/2. The shear directions determined have a subhorizontal orientation, and are presented as a rose diagram in Fig. 7(a).

*Transition zone*

The transition zone represents the margin of the Bergen Arc Shear Zone and has a thickness of approximately 30 m. It shows structures indicating a general increase in superimposed dextral shear towards NE and structurally downwards, although this superimposition is strongly heterogeneous (indicated by the curve on Fig. 3). This zone consists of alternating zones of phyllite, garnet–amphibole–mica-schist and mylonite with lesser amounts of amphibolite, psammite and local thin ultramylonites. Quartz-rich and feldspar-rich lithologies were less affected by the later phase of shear than mica-rich lithologies. The structural development is more complex than in the upper zone due to the superimposed dextral shear on asymmetric structures which indicated sinistral shear (Fig. 3).

In spite of this increase in complexity, many of the same structural features can still be recognised as described in the upper zone. Shear bands ($SB_1$) and associated curved/inclined foliation ($SI_1$) indicative of sinistral movement can frequently be observed in this zone, but are less abundant than in the upper zone. However, the $\beta$ angle between these structural elements is reduced, and most measurements are between 120 and 140°. The mean is decreased to 129.5° associated with a slight increase in standard deviation (Fig. 6b). Although the shear bands are clearly indicative of sinistral movements, close inspection of thin sections of these structures reveals that the $SI_1$ foliation is locally folded (Fig. 5b). These folds are often asymmetric with a dextral vergence. The sinistral shear bands are also often enriched in opaque minerals. The reduction in $\beta$ and the associated folding of the $SI_1$ are interpreted as a result of superimposed dextral shear on inherited $SB_1$ and $SI_1$, as discussed later.

Folded quartz lenses show a great variety of shapes in this zone. A common shape is a tighter variation of the sigmoidal shape in the upper zone (Figs. 3, 5c & d). These shapes are interpreted to have been formed by superimposed dextral shear on asymmetric boudins originated during earlier sinistral shear. Folded quartz veins show more complex geometries than the lenses, and they often have an asymmetry indicative of dextral shear (Fig. 5e). These folds are open to tight and commonly have a thin and a thick set of limbs similar to the gentle folds or asymmetric pinch-and-swells in the upper, sinistral zone. Thus, these are suggested to have originated as asymmetric pinch-and-swells during sinistral shear, later being modified and tightened during the superimposed dextral shear.

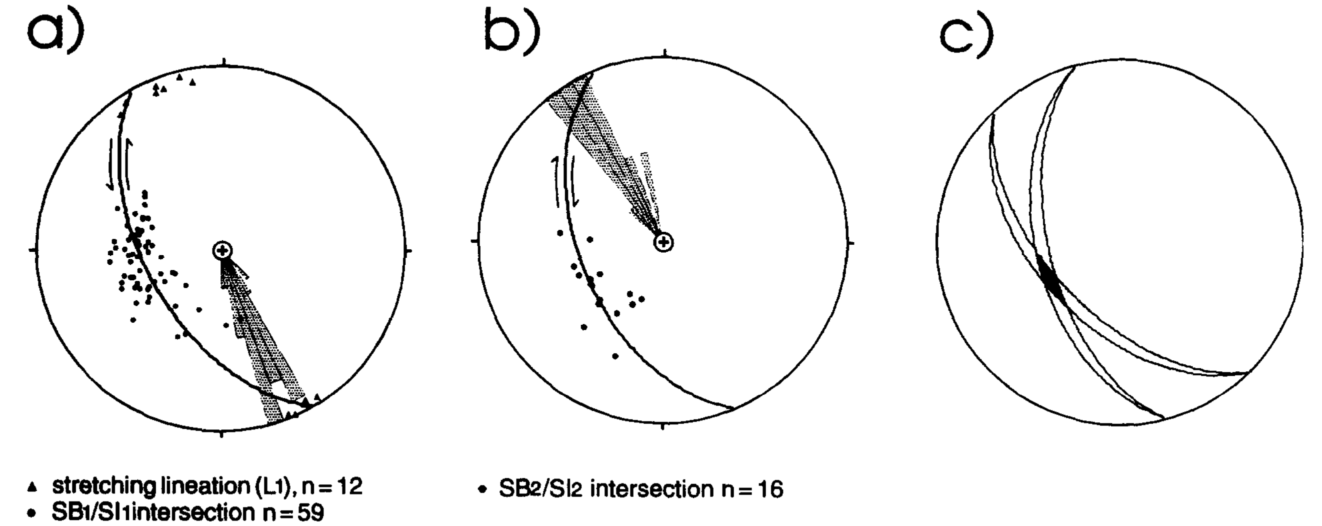


Fig. 7. (a) Determined shear directions from the upper (sinistral) zone plotted as a rose diagram. Stereogram is equal area/lower hemisphere. Great circle represents inferred shear plane. See text for discussion. (b) Same as (a) for the lower (dextral) zone. (c) Accuracy considerations for the $SB_1/SI_1$ intersection. Shaded area represents the range of variation ($\pm 13°$) for an inaccuracy of $\pm 3°$ in the dip measurement.

The hingelines to the folded quartz lenses are commonly located at the transition from the central parts to the thin tails, and those of the veins at the transition from thin to thick limbs. The hinge lines are interpreted to have originated as the intersections between $SB_1$ and $SI_1$ during sinistral shear and were rearranged and modified during the later dextral shear. Hinge lines of folded quartz lenses and veins show a relatively good girdle distribution with the best fit great circle corresponding to the mean of the axial planes (Fig. 4d). The majority of these hingelines have an orientation similar to the $SB_1/SI_1$ intersection in the upper, sinistral zone (Fig. 7a).

Locally, crenulations are developed by folding of the $S_1$ and $SI_1$ foliations (Fig. 5b). $S_1$ is also folded on a larger scale with wavelengths of 3–8 m and amplitudes up to 0.5 m, and this is expressed by the dispersion of the poles to $S_1$ (Fig. 4c). These folds commonly show a dextral vergence, and an axial plane cleavage ($S_2$) is locally developed which is strongest in the hinge zones. They are consequently interpreted as a result of the later dextral phase of shear. Shear bands indicating dextral shear are also developed locally in thin zones.

*Lower zone—dextral kinematic indicators*

The lower zone is within the Bergen Arc Shear Zone which was active during late/post Caledonian top-to-NW extension. Phyllite is the dominant lithology with occasional psammitic horizons. Garnet is not observed in this zone. The main structural elements in the lower zone, at the outcrop scale, look in general like a mirror image of the structural elements of the upper, sinistral zone (Fig. 3). Zones with a single planar structure ($S_1$) separate zones with two structures, here called $SI_2$ and dextral shear bands ($SB_2$) indicating dextral sense of shear. Locally, subhorizontal lineations are developed on $SB_2$ and $SI_2$. The shear bands are developed in mica-rich lithologies whereas quartz/feldspar-rich zones commonly have only one planar structure which is correlated with $S_1$ in the upper zone. Locally within the quartz/feldspar-rich zones shear bands indicating sinistral shear ($SB_1$) are preserved. These are interpreted as remnants from the earlier phase of shear. Therefore, the superimposed dextral shear in this zone is also heterogeneous as indicated by the curve on Fig. 3. (Note that this figure is out of scale and the thicknesses of the zones of subordinate superimposed shear are exaggerated.) In general, the dextral shear bands occur where the quartz lenses and veins are tightly to isoclinally folded. $S_1$ is (in contrast to the upper zone) commonly crenulated in the lower zone, and $S_1$ measurements in Fig. 4(e) represent the enveloping surface. The crenulations of $S_1$ do not show any consistent vergence.

The planar fabric between the dextral shear bands, called $SI_2$, is of two types: a composite cleavage $SI_{C2}$ and a penetrative $SI_{P2}$ (Fig. 3). $SI_{C2}$ is different from the simpler $SI_1$ in the upper zone. It is also developed in the transition zone associated with the local dextral shear bands, and consists of two elements: a discrete cleavage enriched in opaque minerals separating domains of a zonal crenulation cleavage (Figs. 5f & g). The zonal crenulation cleavage is characterised by folded mica aggregates and shows variable development and orientation due to complex fold geometries. The zonal crenulation cleavage is subparallel to the discrete cleavage. $SI_{C2}$ is thought of as originating by dextral shear superimposed on earlier sinistral structures (see later). Similar structures related to superimposed shear with opposite directions have been described from the Ofoten area in northern Norway (Rykkelid & Andresen 1994). The penetrative $SI_{P2}$ in the phyllites of the lower zone is similar to $SI_1$ in the garnet–mica-schists of the upper zone, although the $SI_{P2}$ fabric is more fine-grained. The $SI_{P2}$ is interpreted to represent a higher amount of superimposed dextral shear, resulting in obliteration of the earlier fabrics.

The mirror image symmetry of the main structural elements in the upper and lower zones also finds its expression in the stereograms from the two zones (Figs. 4a & e). Also in the lower zone, the clusters of $SB_2$ and $SI_2$ poles are distributed symmetrically around the cluster of the $S_1$ poles. The $S_1$ foliation has roughly the same orientation in the two zones. $SI_2$ in the lower zone has the same orientation as the $SB_1$ in the upper zone, and the $SB_2$ of the lower zone the same orientation as $SI_1$ of the upper zone. The obtuse angle between the dextral $SB_2$ and $SI_2$ is in the range of 135–155°.

The quartz lenses and veins show an increased degree of folding from the upper zone through the transition zone to the lower zone, where both are tightly to isoclinally folded. $SI_2$ is axial planar to these folds. Although the fold geometries in general are complex, two distinct features of these folds can be observed. Firstly, sigmoidal quartz veins occur between the shear bands and the edges of these are folded in the opposite direction to drag of $SI_2$ towards the shear bands (Figs. 5h & i). The tails of the lenses are folded subparallel to the central part. Since the shear bands are tangents to the hinges of the folded quartz lenses, the latter had a controlling effect on the development of the shear bands. Locally, isoclinally folded quartz veins are cut by the new dextral shear bands. Secondly, as in the transition zone, the folded quartz veins are characterised by one set of limbs being thinner than the other. It is suggested that both these features are a result of the increased effect of dextral shear superimposed on inherited sinistral asymmetric boudins and pinch-and-swell structures.

Within the lower zone, one example of imbricated psammite bands is observed, and the configuration of these indicates sinistral sense of shear with the present orientation (Fig. 3). However, close inspection of shear bands in the zones between the slices of psammite, indicates that the latest movements were dextral. In this case, the effect of the first phase of sinistral shear was the largest, and the later phase of dextral shear was relatively weak and did not transport the slices back to the pre-sinistral–shear position. This is interpreted as a small-scale field analogue of the regional Mode I extension of Fossen (1992), whereby Caledonian SE-directed thrusts were reactivated during late/post Caledonian top-to-NW extension.

The structural development within this zone and across the transition zone suggests that the first sinistral phase of shear also affected these rocks with the same sense of shear as in the upper zone. The shear plane in the lower zone is assumed to be parallel to the mean $S_1$ foliation (157/52 SW), although there is some discrepancy between this and the plane bisecting the acute angle between the $SB_2$ and $SI_2$ (141/52 SW). Due to the folding of $S_1$ and poorly developed stretching lineations, the shear plane and shear direction are less constrained than in the upper zone. The shear direction during the later dextral phase of shear is determined with the use of the geometric relationship between shear bands and $SI_2$ as in the upper, sinistral zone. The determined shear direction has a mean of 329/4, and the sense of shear is top-to-NW (Fig. 7b). The shear direction is thus approximately the same as in the sinistral zone from the first phase of deformation, whereas the sense of shear is opposite.

## 2D-MODEL — 'SHEAR BOX' EXPERIMENT

The previously described observations are interpreted as illustrating how dextral shear progressively deforms structures inherited from an earlier sinistral phase of shear. The senses of shear during the two phases were approximately opposite whilst the shear plane and shear direction were approximately the same. This implies that some of the analysis of these structures can be performed in 2D.

To obtain a simplified impression of the geometrical changes during superimposed dextral shear on inherited structures from sinistral shear, a 'shear-box' simulation was carried out (Fig. 8a). This was performed using a PC drawing program. A set of shear bands ($SB_1$) with associated curved/inclined foliation ($SI_1$) indicating sinistral shear were drawn on a rectangle in a Cartesian co-ordinate frame. The obtuse angle $\beta$ between the two planar structures is approximately 155° and they are oriented symmetrically about the shear plane. This rectangle and its structures were then deformed by dextral ideal simple shear parallel to the X-axis. During this 'shear box' experiment, both $SB_1$ and $SI_1$ behave as passive markers and therefore rotate according to the relationships given in the Appendix.

This 'shear-box' experiment shows that for moderate dextral superimposed shear ($\gamma_D = 1$ and $\gamma_D = 2$, where $\gamma_D$ is defined as $-\gamma$, i.e. positive $\gamma_D$ implies dextral shear) only minor modification of the inherited sinistral structures takes place. Close inspection reveals only a slight reduction in $\beta$ and a reduction in the distance between the shear bands. The geometry of these structures is still likely to be interpreted as only the result of sinistral shear. With increasing amount of dextral shear (e.g. $\gamma_D = 4$) the effect of dextral superimposition gets more pronounced. There is a dramatic reduction in $\gamma$, and the distance between the shear bands is further reduced.

The change in $\beta$ can be expressed as a function of shear strain $\gamma_D$ assuming passive rotation in ideal simple shear. This function has been plotted for an initial $\beta = 160°$, and for $SB_1$ and $SI_1$ being symmetric about the shear plane (Figs. 8b & c). Another feature of the dextral superimposition on inherited sinistral structures revealed by the 'shear-box' experiment is the reduction in the distance $d$ between the shear bands. This relationship can also be expressed as a function of shear strain (Fig. 8c and the Appendix).

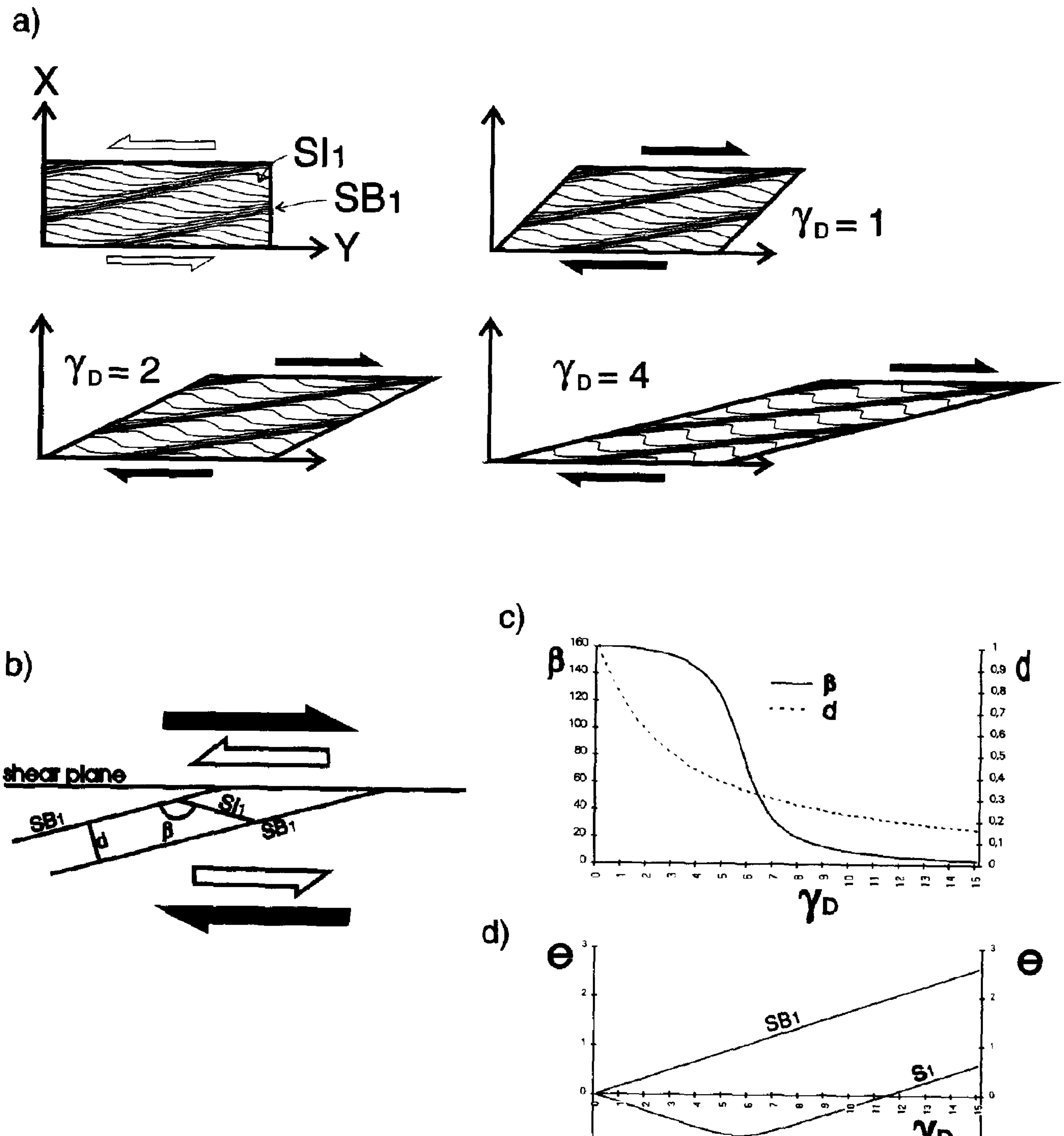


Fig. 8. (a) 'Shear-box' experiment performed using a drawing program on a personal computer by superimposing dextral simple shear on earlier shear bands ($SB_1$) and curved/inclined foliation ($SI_1$) resulting from sinistral shear. See text for discussion. (b) Geometrical elements for analysis of superimposed dextral simple shear on inherited $SB_1$ and $SI_1$. (c) Change in obtuse angle $\beta$ between $SB_1$ and $SI_1$ (solid line) and distance d between shear bands (stippled) with increasing superimposed dextral shear. (d) Elongation of $SB_1$ and $SI_1$ as a function of $\gamma_D$. See Appendix for derivation of functions.

$SI_1$ and $SB_1$ are oriented with different initial angles to the shear plane. During ideal simple shear, the lengths of these structural elements will change with increasing superimposed dextral shear (Fig. 8d, cf. Ramsay & Huber 1983). The shear bands are initially oriented in the extensional field of the instantaneous strain ellipse and will undergo continuous extension with increasing $\gamma_D$. $SI_1$ starts with an orientation in the contractional field and will undergo a period of shortening before it rotates into the extensional field. This phase of shortening is suggested to have had an effect on the microstructures observed. Firstly, microfolds of $SI_1$ are observed between the sinistral shear bands in the transition zone associated with the decrease in $\beta$. Secondly, this can contribute to the development of the zonational crenulation cleavage.

The deformation in this analysis is ideal simple shear of an isotropic medium in 2D where $SB_1$ and $SI_1$ behave as passive markers during the deformation. This deformation mechanism is not likely to be realistic in the presented field example. Firstly, the starting material for the superimposed dextral shear is clearly anisotropic containing two different planar fabrics. Secondly, several recent publications have concluded that deformation in many shear zones may be general non-coaxial deformation and not ideal simple shear (e.g. Passchier 1987, Hanmer 1990, Masuda *et al.* 1995). However, the model demonstrates some of the general geometrical consequences of modifying sinistral shear bands by dextral simple shear.

## DISCUSSION

### *Progressive dextral superimposition on inherited sinistral structures*

The observations of fabrics and structures along the Askvik shore section from the upper through the transition and lower zones, are interpreted to represent successive stages in the progressive superimposition of dextral shear on inherited sinistral structures. The shear plane and shear direction are suggested to have been the same during the two phases of deformation, but the sense of shear was reversed. These observations in addition to

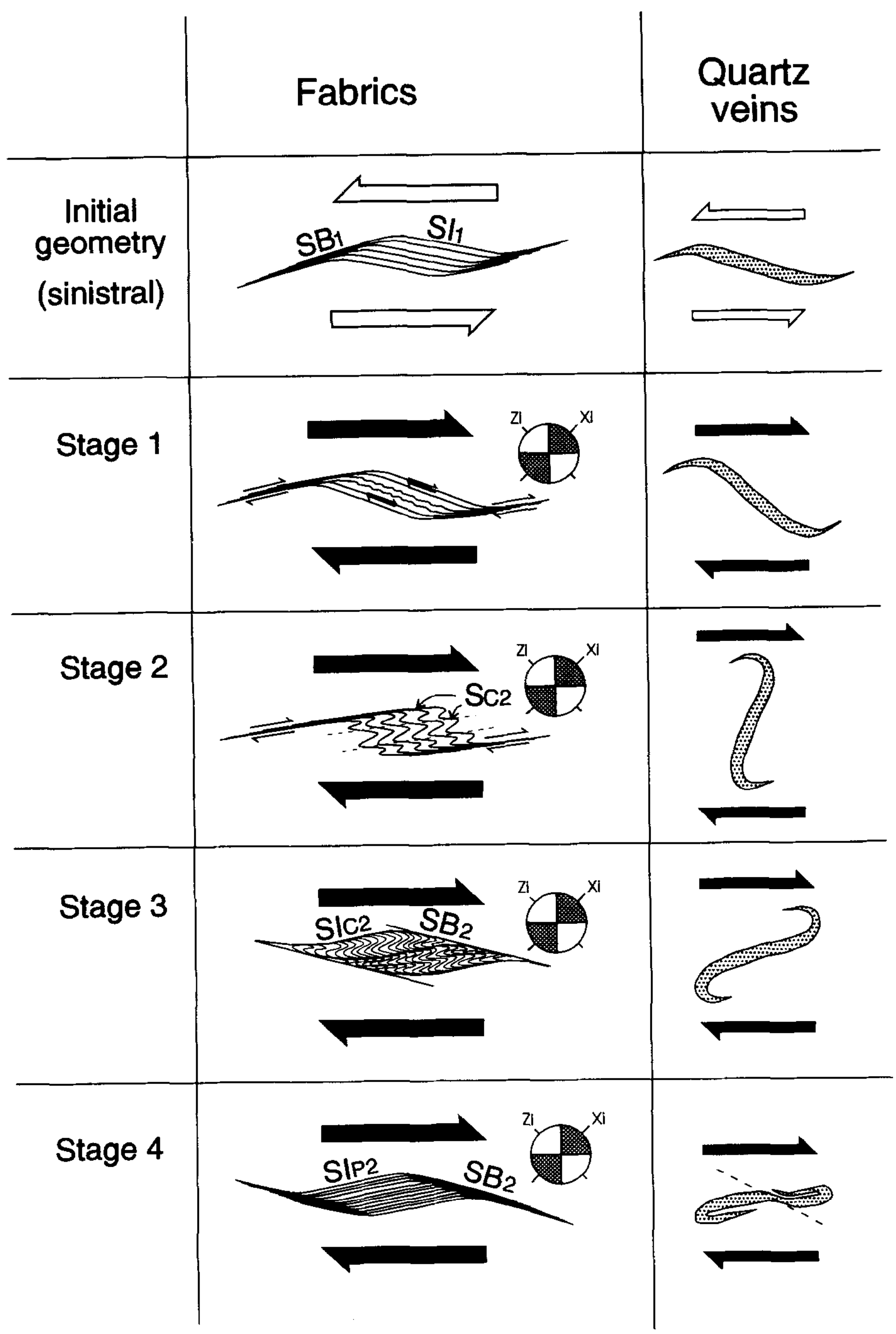


Fig. 9. Progressive dextral superimposition on inherited sinistral shear bands ($SB_1$) with associated curved inclined foliation $SI_1$ and asymmetric boudins. See text for discussion.

the simple geometric analysis above, suggest the following evolutionary model (Fig. 9).

*Stage 1*

Stage 1 is expressed as a reduction of the obtuse angle $\beta$ between the sinistral shear bands ($SB_1$) and the curved/inclined foliation ($SI_1$). The reduction of $\beta$ is a result of the clockwise rotation of both $SB_1$ and $SI_1$, where the latter has the greatest rotation rate. Quartz veins and lenses are only very slightly folded, and in general only minor modifications of the inherited structures occur. The geometric analysis (Fig. 8) also indicates that these may take up a significant amount of dextral shear prior to any major change in $\beta$. Both $SB_1$ and $SI_1$ are orientated at a low angle to the shear plane of the superimposed dextral deformation. Thus they are potential slip planes, and the deformation during stage 1 is likely to be at least partly taken up by slip along these pre-existing surfaces.

This implies that observations of structures resulting from moderate dextral superimposition of inherited sinistral structures may still be interpreted in the field as resulting from only one phase of shear. However, observations in thin-sections show that $SI_1$ is locally folded between the shear bands, associated with the reduction of $\beta$. This is a response to $SI_1$ having an initial orientation in the shortening field of the instantaneous strain ellipse during the superimposed dextral shear. These microfolds occur only locally, and this supports the suggestion that the deformation was mainly taken up by slip along the pre-existing foliations.

*Stage 2*

The composite cleavage ($S_{C2}$) is inferred to develop during stage 2. During stage 1 the dextral shear is partly taken up by slip along the $SI_1$ foliation surfaces while these rotate clockwise. Subsequently, due to the superimposed dextral shear, $SI_1$ is rotated to an orientation where slip is less favourable and eventually stops. $SI_1$ is still in the shortening field of the instantaneous strain ellipse. This defines the transition to stage 2 where the folding of $SI_1$ increases and develops into a zonal crenulation cleavage, which can be compared with the reverse crenulation cleavage of Dennis & Secor (1987) and the kink bands developed in shear experiments on artificial slates by Williams & Price (1990). However, in this case the crenulations are developed in narrow parallel zones separated by the discrete cleavage, which develops contemporaneously by enhancement of the sinistral shear bands. Similar fabrics interpreted as a result of top-to-W shear superimposed on top-to-E fabrics have been described from the Ofoten area in the Northern Norwegian Caledonides by Rykkelid & Andresen (1994) and from southern Norway (Fossen, 1992).

The folding of quartz veins and lenses becomes more pronounced during stage 2 (Fig. 9). The quartz lenses show characteristic sigmoidal shapes (Fig. 5c). These are interpreted to have originated as asymmetric boudins during the phase of sinistral shear. Both the central parts and the thin tails of the boudins rotate during superimposed dextral shear, but the rotation rate is higher for the central part. The folded quartz veins often have one set of limbs thinner than the other. They are interpreted to have originated during sinistral shear as asymmetric pinch-and-swell structures, which also can be described as gentle folds. During dextral shear these 'folds' were amplified by a higher rotation rate of the thicker limb. The detailed deformation mechanism during this rotation and folding is not the focus of this paper, but it is assumed that the folding can be explained by components of buckling and passive rotation.

Examples of back-folding are reported from several places in the Norwegian Caledonides (e.g. Osmundsen & Andersen 1994, Fossen & Holst 1995). Foliations formed during the Caledonian top-to-SE deformation were orientated in the shortening field of the instantaneous strain ellipse during the subsequent top-to-NW extension. This is commonly interpreted to have resulted in the NW-vergent fold pattern. The formation of the zonal crenulation cleavage is interpreted to be a microscopic example of back-folding, and the folding of the quartz veins and lenses is a macrosopic example of the same phenomenon. However, the curved/inclined foliation ($SI_1$) had, in the present case, a significant effect on the structures developed during the superimposed reversed shear. Asymmetrically boudinaged quartz veins had variable geometries and orientations inherited from the sinistral phase. In addition to marked competence contrast to the mica-rich matrix, this resulted in the great variety and complexity of the fold geometry resulting from the later dextral shear.

*Stage 3*

Stage 3 is characterized by the initiation of shear bands indicative of dextral sense of shear (Fig. 9) which are observed locally in the transition zone and which dominate within the Bergen Arc Shear Zone. Between the dextral shear bands ($SB_2$) at stage 3, the curved/inclined foliation is of the composite type ($SI_{C2}$). At this stage, the quartz lenses and veins become tightly to isoclinally folded (Fig. 5i). Critical for recognizing this as superimposed dextral shear on inherited sinistral asymmetric structures are the observations of these folded quartz lenses in addition to the composite cleavage ($SI_{C2}$).

*Stage 4*

At higher dextral shear strain the remains of the earlier sinistral phase of shear is completely obliterated and no remains of the earlier phase of deformation are present. The earlier sinistral shear bands ($SB_1$) and now intensely folded $SI_1$ become close to parallel and it is impossible to distinguish between the two. They develop and rotate into the new penetrative $SI_{P2}$ fabric between shear bands indicative of dextral shear ($SB_2$). The dextral shear bands

($SB_2$) also cut through the isoclinally folded quartz lenses and veins (Fig. 9).

*Heterogeneous, superimposed shear*

The superimposed, dextral shearing, whose effects are so well exposed along the Askvik shore section, was heterogeneous, and the effect of this was to interleave zones with different structural characteristics as in the transition zone. This can be illustrated by assuming a heterogeneous simple shear profile superimposed on shear bands ($SB_1$) and associated curved inclined foliation ($SI_1$) formed during sinistral non-coaxial deformation (Fig. 10). The shear plane and shear direction are the same, but the sense of shear is opposite during the two phases, as in the presented field example. In zones of relative low dextral shear, inherited sinistral shear bands are likely to be preserved (stage 1). The frequency distribution of $\beta$ in the transition zone (Fig. 6b) is interpreted as a result of a heterogeneous strain profile. Heterogeneous shear strain has here resulted in the decrease in the mean $\beta$ associated with an increase in the standard deviation relative to the upper zone (Fig. 6a).

In zones of moderate superimposed dextral shear, crenulations of $SI_1$ foliation and the composite cleavage will develop (stage 2). Shear criteria within these zones will be asymmetric folding of the earlier fabric with a dextral vergence. Zones of higher superimposed shear will develop shear bands indicative of dextral shear (stage 3), and eventually the earliest fabric is obliterated and rotated into $S_2$. Therefore, a pattern of alternating dextral and sinistral shear bands as across the margin of the Bergen Arc Shear Zone can be explained by a two-phase bulk simple shear model. In this case, several related planar structures are present, e.g. $S_1$, $SI_1$, $SB_1$ (sinistral), $SI_2$ and $SB_2$ (dextral). Direct evidence that two phases of deformation took place will only be found in a rather narrow interval (stages 2 and 3).

Conflicting sense of shear has been described in several earlier papers, and possible explanations for this are as follows. (1) A combination of general non-coaxial shear and strain partitioning resulting in volumes of rock which suffered bulk coaxial deformation during one phase of deformation (e.g. Bell & Johnson 1992). (2) Conjugate shear bands may be formed locally during one phase of bulk simple shear when the foliation is inclined to the shear zone (Harris & Cobbold 1985). (3) Multi-stage deformation histories where the conflicting senses of shear have been formed during different parts of the history (Bell & Johnson 1992). It is suggested that the presented field example, where sinistral and dextral shear bands are localized to parallel zones of different lithologies, are a variation of the third. The applied model involves a two-phase deformation history involving bulk simple shear with the shear plane and shear direction being the same and the sense of shear being opposite.

Microstructural investigations are essential to distinguish between the different models for conflicting senses of shear. Diagnostic for a two-phase simple shear model would be the difference in the fabric between the shear bands, where the later set show a $SI_{C2}$ composite cleavage and the earlier a simpler $SI_1$ fabric. Also typical for superimposed shear will be a dominance of one sense of shear in some rock types and the opposite in other. In contrast, strain partitioning (in general, non-coaxial shear) results in both senses of shear being present in zones of the same lithology. In the investigated field example, sinistral shear bands are preserved within the Bergen Arc Shear Zone in quartz/feldspar rich lithologies, whereas superimposed dextral shear is restricted to the micaceous lithologies. This may also suggest that the conditions were different during the two phases of deformation.

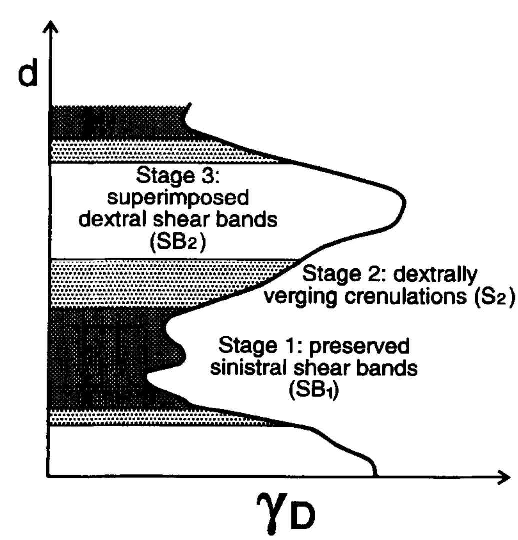


Fig. 10. Schematic strain profile across a zone of earlier sinistral shear, where the superimposed shear is dextral.

## CONCLUSIONS

The field example and geometric analysis presented have shown that when shear zones have been affected by two phases of shear, complex structural relations develop, even when the shear plane and shear direction were the same and the sense of shear was opposite during the two phases. In several orogens, like the Scandinavian Caledonides, late/post orogenic extension has modified earlier contractional fabrics. This results in complex structural development both on a large scale involving the whole crust, and on a small scale within reactivated shear zones like the one described here, where the kinematics should be evaluated with care.

*Acknowledgements*—A.G. Milnes, H. Fossen and N. Odling, in addition to the reviewers T. Blenkinsop and S. Hanmer, are thanked for critical comments and suggestions which have improved the manuscript significantly. J. Ellingsen and E. Lier are thanked for drafting the figures.

## REFERENCES


Andersen, T. B. & Jamtveit, B. 1990. Uplift of deep crust during orogenic extensional collapse; a model based on field studies in the Sogn-Sunnfjord. region of western Norway. *Tectonics* 9, 1097–1111.

Andersen, T. B., Skjerlie, K. P. & Furnes, H. 1990. The Sunnfjord Melange; evidence of Silurian ophiolite accretion in the West Norwegian Caledonides. *J. geol. Soc. Lond* **147**, 59–68.

Bell, T. H. & Johnson, S. E. 1992. Shear sense: a new approach that resolves conflicts between criteria in metamorhic rocks. *J. metamorph. Geol.* **10**, 99–124.

Berthé, D., Choukroune, P. & Jegouzo, P. 1979. Orthogneiss, mylonite and non-coaxial deformation of granites: the example of the South Armorican Shear Zone. *J. Struct. Geol.* **1**, 31–42.

Chauvet, A. & Séranne, M. 1989. Microtectonic evidence of Devonian extensional westward shearing in Southwest Norway. In: *The Caledonide Geology of Scandinavia* (edited by Gayer, R.A.). Graham & Trotman, London, 245–254.

Dennis, A. J. & Secor, D. T. 1987. A model for the development of crenulations in shear zones with applications from the Southern Appalachian Piedmont. *J. Struct. Geol.* **7**, 809–817.

Dunning, G. R. & Pedersen, R.B. 1988. U/Pb ages of ophiolites and arc-related plutons of the Norwegian Caledonides: implications for the development of Iapetus. *Contr. Miner. Petrol.* **98**, 13–23.

Fossen, H. 1992. The role of extensional tectonics in the Caledonides of south Norway. *J. Struct. Geol.* **15**, 1033–1046.

Fossen, H. & Holst, T.B. 1995. Northwest-verging folds and the northwestward movement of the Caledonian Jotun Nappe, Norway. *J. Struct. Geol.* **17**, 3–15.

Furnes, H., Roberts, D., Sturt, B., Thon, A. & Gale, G. 1980. Ophiolite fragments in the Scandinavian Caledonides. *Proc. Int. Ophiolite Symp. Nicosia Cyprus 1979*. 295–307.

Færseth, R. B., Thon, A., Larsen, S. G., Sivertsen, A. & Elvestad, L. 1977. Geology of the Lower Palaeozoic Rocks in the Samnanger-Osterøy Area, Major Bergen Arc, Western Norway. *Norges geol. unders.* **334**, 19–58.

Goldstein, A. F. 1988. Factors affecting the kinematic interpretation of asymmetric boudinage in shear zones. *J. Struct. Geol.* **7**, 707–715.

Griffin, W. L., Austrheim, H., Brastad, K., Bryhni, I. Krill, A. G., Krogh, E. J. Mørk, M. B. E., Qvale, H. & Tørudbakken, B. 1985. High-pressure metamorphism in the Scandinavian Caledonides. In: *The Caledonian Orogeny—Scandinavia and related areas* (edited by Gee, D. A. & Sturt, B. A.). Wiley, New York, 783–801.

Hanmer, S. 1986. Asymmetrical pull-aparts and foliation fish as kinematic indicators. *J. Struct. Geol.* **8**, 111–122.

Hanmer, S. 1990. Natural rotated inclusions in non-ideal shear. *Tectonophysics* **149**, 245–255.

Hanmer, S. & Passchier, C. 1991. Shear-sense indicators: a review. *Geol. Surv. Pap. Can.* **90**, 17.

Harris, L. B. & Cobbold, P. R. 1985. Development of conjugate shear bands during bulk simple shearing. *J. Struct. Geol.* **7**, 37–44.

Hossack, J. R. 1984. The geometry of the listric faults in the Devonian basins of Sunnfjord, Western Norway. *J. geol. Soc. Lond.* **141**, 629–637.

Kolderup, C. F. & Kolderup, N. H. 1940. Geology of the Bergen Arcs. *Bergen Museums Skrifter* **20**, 137 pp.

Masuda, T., Michibayashi, K. & Ohta, H. 1995. Shape preferred orientation of rigid particles in a viscous matrix: re-evalution to determine kinematic parameters of ductile deformation. *J. Struct. Geol.* **17**, 115–129.

Milnes, A. G. & Koestler, A. G. 1985. Geological structure of Jotunheimen, southern Norway (Sognefjell–Valdres cross-section). In: *The Caledonian Orogeny—Scandinavia and related areas* (edited by Gee, D. A. & Sturt, B. A.). Wiley, New York, 457–474.

Milnes, A. G., Dietler, T. N. & Koestler, A. G. 1988. The Sognefjord north shore log—a 25 km depth section through the Caledonized basement in western Norway. *Norges geol. unders. Spec. Publ.* **3**, 114–121.

Naterstad, J., Andresen, A. & Jorde, K. 1973. Tectonic succession of the Caledonian nappe front in the Haukeli–Røldal area, southwest Norway. *Norges geol. unders.* **292**, 1–20.

Norton, M. G. 1986. Late Caledonian extension in the western Norway: a response to extreme crustal thickening. *Tectonics* **5**, 192–204.

Norton, M. G. 1987. The Nordfjord–Sogn Detachment, West Norway. *Norsk Geologisk Tidsskrifit* **67**, 93–106.

Osmundsen, P. T. & Andersen, T. B. 1994. Caledonian compressional and late-orogenic extensional deformation in the Staveneset area, Sunnfjord, Western Norway. *J. Struct. Geol.* **16**, 1385–1402.

Passchier, C. W. 1987. Stable position of rigid objects in non-coaxial flow—a study in vorticity analysis. *J. Struct. Geol.* **9**, 679–690.

Platt, J .P., Vissers, R. L. M. 1980. Extensional structures in anisotropic rocks. *J. Struct. Geol.* **2**, 397–410.

Ramsay, J. G. 1980. Shear zone geometry: a review. *J. Struct. Geol.* **2**, 83–99.

Ramsay, J. G. & Huber, M. I. 1983. *The Techniques of Modern Structural Geology. Vol 1: Strain Analysis*. Academic Press, London, 307 pp.

Reusch, H., 1882. Silurfossiler and Pressede Konglomerater i Bergensskifrene. Kristiania (Oslo) 152 pp.

Roberts, D. & Sturt, B. A. 1980. Caledonian deformation in Norway. *J. geol. Soc. Lond.* **137**, 241–250.

Ryan, P. D. & Skevington, D. 1976. A Re-interpretation of the Late-Ordovician–Early Silurian Stratigraphy of the Dyvikvågen and Ulven–Vaktdal areas, Hordaland, Western Norway. *Norges geol. unders.* **324**, 1–19.

Rykkelid, E., Andresen, A. 1994. Late Caledonian extension in the Ofoten area, northern Norway. *Tectonophysics* **231**, 157–169.

Séranne, M. & Seguret, M. 1987. The Devonian basin of western Norway: tectonics and kinematics of an extending crust. In: *Contineral Extensional Tectonics* (edited by Coward, M.P., Dewey, J.F. & Hancock, P.L.). *Spec. Publs geol. Soc. Lond* **28**, 537–548.

Séranne, M., Chauvet, A. & Faure, J. L. 1991. Cinématique de l'extension tardi-orogénique (Devonien) dans les Calédonides Scandinaves et Britanniques. *C. R. Acad. Paris* **313**, *Sèrie II*, 1305–1312.

Skjerlie, F. J. 1969. The Pre-Devonian rocks in the Askvoll–Gaular area and adjacent districts, western Norway. *Norges geol. unders.* **258**, 325–359.

Sturt, B. A. & Thon, A. 1976. The age of orogenic deformation in the Swedish Caledonides. *Am. J. Sci.* **276**, 385–390.

Sturt, B. A. & Thon, A. 1978. Caledonides of Southern Norway. In: *IGCP Project 27. Caledonide–Appalachien Orogen of the North Atlantic Region. Geol. Surv. Canada*, Paper **78-13**, 39–47.

Swensson, E. & Andersen, T. B. 1991. Contact relationships between the Askvoll group and the basement gneisses of the Western Gneiss Region (WGR). *Norsk Geologisk Tidsskrift* **71**, 15–27.

Thon, A. 1985. The Gullfjellet Ofiolite Complex and the structural evolution of the Bergen Arcs, Western Norway. In: *The Caledonian Orogeny—Scandinavia and related areas* (edited by Gee, D. A. & Sturt, B. A.). Wiley, New York, 671–677.

Wennberg, O. P. & Milnes, A. G. 1994. Interpretation of kinematic indicators along the northeastern margin of the Bergen Arc System: a preliminary field study. *Norsk Geologisk Tidsskrift* **74**, 166–173.

Williams, P. F. & Price, G. P. 1990. Origin of kinkbands and shear-band cleavage in shear zones: an experimental study. *J. Struct. Geol.* **12**, 1145–1164.

White, S. H., Burrows, S. E., Carreras, J., Shaw, N. D. & Humphreys, F. J. 1980. On mylonites in ductile shear zones. *J. Struct. Geol.* **2**, 175–187.


## APPENDIX

The obtuse angle $\beta$ between shear bands ($SB_1$) and curved/inclined foliation ($SI_1$) will change as a result of superimposition of simple shear. The initial angle $\beta$ can be expressed as:

$$\beta = \alpha_2 - \alpha_1. \quad (A1)$$

After superimposed dextral shear strain, i.e. in the deformed state, the angle $\beta'$ becomes

$$\begin{aligned}\beta' &= \alpha'_2 - \alpha'_1 \\ &= \cot^{-1}(\cot\alpha_2 + \gamma D) - \cot^{-1}(\cot\alpha_1 + \gamma D)\end{aligned} \quad (A2)$$

where

$$\gamma D = -\gamma. \quad (A3)$$

Another geometrical consequence of dextral modification of inherited sinistral shear bands ($SB_1$) is a reduction in the distance between the shear band. The initial orthogonal distance d can be expressed as

$$d = x\sin\alpha \quad (A4)$$

where $\alpha$ is the initial angle between the shear plane and $SB_1$. During simple shear the distance $x$ between the parallel planes in the shear plane will be constant and the distance d′ between the shear bands in the deformed state is given by

$$d' = x^{*}\sin\alpha' = \frac{d * \sin\alpha'}{\sin\alpha}. \quad \text{(A5)}$$

$\alpha'$ is a function of superimposed dextral shear–strain $\gamma$ and is given by (Ramsay & Huber, 1983):

$$\cot\alpha' = \cot\alpha - \gamma. \quad \text{(A6)}$$

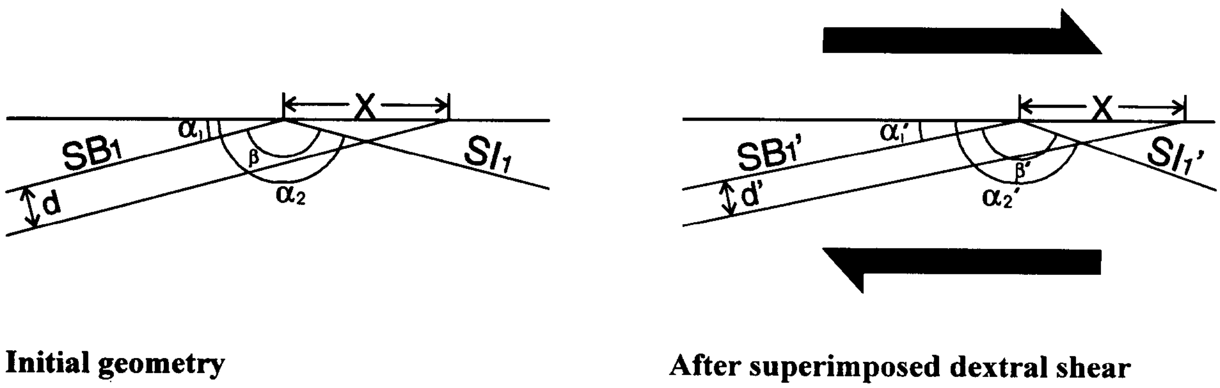


Fig. A1.